



ARTICLE

Effect of PEG Incorporation on Physicochemical and *in vitro* Degradation of PLLA/PDLLA Blends: Application in Biodegradable Implants

Mochamad Chalid^{1,*}, Gifrandy Gustiraharjo¹, Azizah Intan Pangesty¹, Alyssa Adyandra¹, Yudan Whulanza² and Sugeng Supriadi²

¹Department of Metallurgical and Material Engineering, Faculty of Engineering, University of Indonesia, Depok City, 16424, Indonesia

²Department of Mechanical Engineering, Faculty of Engineering, University of Indonesia, Depok City, 16424, Indonesia

*Corresponding Author: Mochamad Chalid. Email: m.chalid@ui.ac.id

Received: 25 September 2022 Accepted: 06 February 2023 Published: 07 June 2023

ABSTRACT

Polyethylene glycol (PEG) was added at different concentrations to the blend of poly(L-lactic acid) (PLLA) and poly(D,L-lactic acid)(PDLLA) to tailor the properties. The differential scanning calorimetry (DSC) measurement showed that all blends were miscible due to shifting a single glass transition temperature into a lower temperature for increasing PEG content. The DSC, FTIR, and XRD results implied the crystallinity enhancement for PEG content until 8 wt%, then decreased at 12 wt% PEG. The XRD result indicated the homo crystalline phase formation in all blends and no stereocomplex crystal. The *in vitro* degradation study indicated that PEG content is proportional to the degradation rate. The highest weight loss after 28 days was achieved at 12 wt% PEG. The FTIR analysis showed a structural evolution overview during hydrolytic degradation, viz. increasing and decreasing crystallinity during 14 days for the blend without and with PEG, respectively. In conclusion, the PEG addition increased crystallinity and degradation rate of the PLLA/PDLLA mixture, but PEG higher amounts led to a decrease in crystallinity, and the weight loss was intensified. This can be useful for tuning PLA-based biomaterials with the desired physicochemical properties and appropriate degradation rates for applications in drug delivery/tissue engineering.

KEYWORDS

PLLA; PDLLA; PEG; crystallinity; degradation

1 Introduction

The use of poly (L-lactic acid) (PLLA) in biomedical applications has been increasing over the past few decades, such as for tissue engineering scaffolds [1,2], drug carriers [3,4], dental niches [5,6], and orthopedic fixation [7,8]. PLLA is biocompatible and biodegradable because the degradation product is safe and non-toxic to humans [9–11]. Its use for bio-absorbable implants also provides a distinct advantage because it eliminates the need for implant removal.

The isotactic structure of PLLA provides beneficial mechanical properties because of the ease of forming a crystalline structure. However, the high crystallinity and slow degradation time [12–14] of PLLA hinder the



technical handling. For the intended application of bone fixation, the flexibility and malleability of the materials must suit the clinical requirements.

To overcome this limitation, several methods are used to enhance the ductility of brittle poly (lactic acid) (PLA). Blending with flexible polymers, e.g., poly (caprolactone) (PCL) [15–18] and poly (glycolic acid) (PGA) [19,20], is commonly used to reduce the rigidity of PLA. However, both PCL and PGA are immiscible with PLLA [21–23]. Therefore mixing the two causes phase separation, which will potentially lead to early implant failure. The brittleness of PLLA can also be altered by blending with amorphous poly (D, L-lactic acid) PDLLA [24]. PDLLA has a random distribution of PLLA and poly (D, lactic acid) (PDLA), which disrupts its stereoregularity [25]. Since both PLLA and PDLLA have similar chemical structures, it is interesting to study the miscibility of the two. PLLA alone degrades very slowly [26], but it is reported that slow degradation is associated with an increased chance of infection [27]. Therefore, the mixture of PLLA and PDLLA was investigated, which is reported to have more rapid degradation [24] within 1 to 3 years [27].

Additionally, plasticizers can be added to improve the malleability by lowering the glass transition temperature (T_g) and controlling the degradation rate in the drug delivery application. Several plasticizers, such as lactic acid oligomer (LAO) [15], citrate esters [28], and PEG [29], have been used for PLA-based mixtures. The latter has been extensively studied because of its vast range of molecular weights [30], biocompatibility [29], and high miscibility with PLA [31], owing to the interaction between the end hydroxyl group of PEG and the carbonyl group of PLA. The addition of PEG into the PLA matrix gives several advantages, such as improving the hydrophilicity of PLA [29], increasing the flexibility and impact toughness [30], and enhancing the crystallization rate [31]. Nevertheless, the influence of PEG on the degradation process of PDLLA and PLLA blends remains poorly understood. In biomedical applications, the degradation process needs to be completely understood because it determines tissue healing and regeneration.

The purpose of this study was to scrutinize the effect of PEG incorporation as a plasticizing agent into the PLLA/PDLLA blend. Moreover, this study aimed to analyze the morphological evolution, thermal characteristics alteration, chemical structure, crystal formation, and degradation behavior using the addition of PEG with various concentrations. PEG was used as the main plasticizing agent, and the PLLA/PDLLA blend ratio was kept constant at 70:30 wt%. Scanning electron microscopy (SEM), differential scanning calorimetry (DSC), x-ray diffraction (XRD), and Fourier transform infrared (FTIR) spectroscopy were conducted to evaluate the changes that occurred to the plasticized polymer blends. Hydrolytic degradation was also performed *in vitro* using phosphate-buffered saline (PBS) media to analyze the mass loss and structural changes.

2 Materials and Method

2.1 Samples Preparation

PLLA (average M_n 30,000), (Sigma-Aldrich, Missouri, USA) and PDLLA (M_n 75,000) (P1691, Sigma-Aldrich, Missouri, USA) with a composition ratio of 70:30 by weight were dissolved in dichloromethane (DCM) (Merck, Darmstadt, Germany) (hereafter denoted as PLA blend). The choice of PLLA and PDLLA compositions was based on research showing that 70:30 is widely used for PLA implant applications because adequate mechanical strength is obtained with appropriate degradation rates at this ratio [27,32]. A polymer/solvent ratio of 1:5 g/ml was used in this study. PEG400 (Merck, Darmstadt, Germany) was added into the blends with a varying degree of content, specifically 0%, 4%, 8%, and 12% by total weight (hereafter denoted as PLA/PEG0, PLA/PEG4, PLA/PEG8, and PLA/PEG12, respectively). The solution blending process was conducted using a magnetic stirrer (C-MAG HS 7, IKA, Malaysia) at room temperature with a mixing speed of 60 rpm. The blending reactor was fluxed with a vacuum suction machine, and nitrogen was continuously streamed into the reactor at a pressure of 3 bar.

The stirring process took place for 1 h until the solution became clear. After 1 h of stirring, the solution was cast into a silicone mold with a dimension of $1 \text{ cm}^2 \times 1 \text{ cm}^2$. The obtained samples were then stored in a vacuum oven at 40°C for 24 h to vaporize the DCM solution from the samples, where they would be trapped inside a liquid-nitrogen-atmosphere chamber. Before characterization, a hot press was used on the samples at a temperature of 200°C for 10 min to obtain a plate shape.

2.2 Characterization

2.2.1 Fourier Transform Infrared (FTIR) Spectroscopy

Chemical structures and functional groups of the samples were characterized using direct measurement by FTIR spectroscopy (Perkin Elmer UATR Two) using the attenuated total reflection method. The solid sample was directly scanned without prior preparation. All samples were scanned using IR spectra of 4000 to 400 cm^{-1} with a resolution of 4 cm^{-1} and 37 scans per sample. FTIR was employed to analyze the structure alteration to examine the intensity ratio from the two band pairs ($I_{1384/1361}$). The $I_{1384/1361}$ value of the blends at 14 and 28 days of degradation was calculated according to the following formula [33]:

$$I_{1384/1361} = \frac{2 - \log(\%T)_{1384}}{2 - \log(\%T)_{1361}} = \frac{A_{1384}}{A_{1361}} \quad (1)$$

with A_{1384} and A_{1361} referring to the absorbance at the 1384 and 1361 cm^{-1} bands, respectively. The %T indicates the percent of transmittance at the respective band.

2.2.2 Differential Scanning Calorimetry (DSC)

The characterization of thermal properties was performed by DSC (Research Center for Biomaterial, Indonesia Institute of Sciences, Indonesia). The sample, approximately 5 mg in weight, was crimped into an aluminum pan with a cover. An empty pan was used as a reference. The first heating was conducted from 0°C to 200°C with a heating rate of $10^\circ\text{C}/\text{min}$ and kept at 200°C for 3 min. The samples were then cooled down to 0°C at a cooling rate of $10^\circ\text{C}/\text{min}$ and reheated for the second run to 200°C with the same heating rate as before. The process was kept under a nitrogen atmosphere throughout the experiment. The degree of crystallinity (X_c) was calculated using the following Eq. (1) [34].

$$X_c = \frac{\Delta H_m - \Delta H_{cc}}{\omega \Delta H_m^0} \times 100\% \quad (2)$$

where ΔH_m and ΔH_{cc} refer to the enthalpies of melting and cold crystallization, respectively, and ω is the weight fraction of PLA in the sample. ΔH_m^0 is the melting enthalpy for 100% crystalline PLA, which is 93.7 J/g [25].

2.2.3 X-Ray Diffraction (XRD)

Crystal structures and orientation of the samples were analyzed by XRD (Research Center for Physics, Indonesia Institute of Sciences, Indonesia). The diffraction angle 2θ was scanned in the range of 10° – 30° with a scanning speed of $5^\circ/\text{min}$ at room temperature. Further analysis of the peak diffraction profile identification and index of crystallinity (I_c) calculation was conducted using Match! (Version 3.12, Crystal Impact, Bonn, Germany).

2.2.4 Hardness Testing

Micro Vickers hardness testing was used to examine mechanical properties (Research Center for Physics, Indonesia Institute of Sciences, Indonesia). The experiment was conducted five times for each specimen at different locations, with each indentation approximately 3 mm away from the previous one.

The force applied in this experiment was 0.03 N for 12 s. Diamond was used as the indenter with an indentation degree of 120°.

2.2.5 Scanning Electron Microscopy (SEM)

Polymer blend samples were fractured into two sections to study the cross-sectional fracture morphology. Gold was sputter-coated on the surface of the fracture with a thickness of 10–20 nm to improve the conductivity of the sample surface. SEM (Inspect F50, FEI Company, Hillsboro, USA) was utilized to visualize the surface morphology.

2.2.6 Weight Loss in Phosphate-Buffered Saline

The degradation behavior of PLA/PEG blends was assessed *in vitro* using PBS. The process was conducted in an incubator to protect the environment from impurities and maintain the temperature at 37°C to imitate the human body condition. All samples were immersed inside a petri dish that was covered with aluminum foil. Mass loss was measured at 0, 7, 14, 21, and 28 days. Every 7 days the PBS solution was changed to maintain a pH of 7.

3 Results and Discussion

3.1 Physicochemical Properties of PLA/PEG Blends

3.1.1 Structural Evolution in the Blending System

Functional group alteration upon PEG addition into the blend was studied by FTIR analysis, as shown in Fig. 1A. Pure PLLA exhibited a sharp peak at 1751 cm⁻¹, which corresponds to C=O stretching of the carbonyl group. Meanwhile, the same functional group displayed a slight shift to 1748 cm⁻¹ in the pure PDLLA sample. The miscibility between PLA and PEG can be observed through intensity evolutions of specific peaks, particularly at 1750 cm⁻¹ (indicative of carbonyl groups [14]). With the higher content of PEG, stronger intermolecular hydrogen bonding occurred because of the rise of terminal hydroxyl fraction in the matrix, as observed with the increase in I_{1750} , as shown in Fig. 1B.

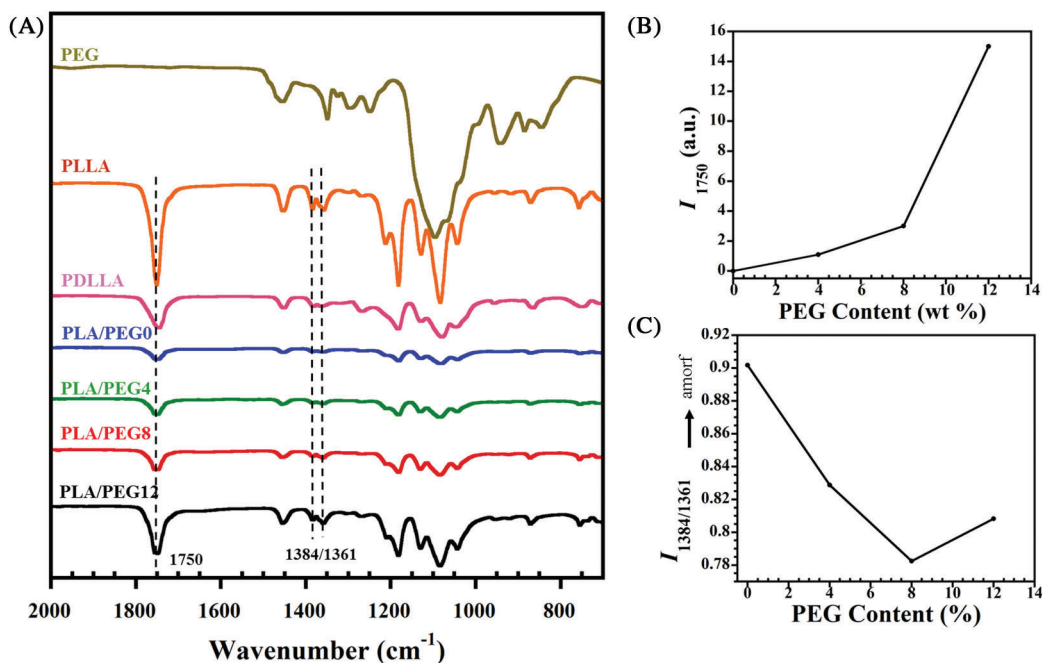


Figure 1: (A) FTIR spectra of PLA/PEG blends. (B) Intensity at the band of 1750 cm⁻¹ (I_{1750}) and (C) $I_{1384/1361}$

Furthermore, the structural evolution due to the PEG incorporation was investigated. Dou et al. [33] reported that the absorbance ratio of the band pairs ($I_{1384/1361}$) changes to a significantly larger value with the increase of amorphous PLLA structures. In this study, we found that the value of $I_{1384/1361}$ also evolves with the increase of PEG content, as seen in Fig. 1C. Compared to that of PLA/PEG0, the $I_{1384/1361}$ greatly decreased with 4% incorporation of PEG. This indicated that the PEG significantly accelerated the crystallization by improving the mobility of PLA chains [31]. The intensity ratio achieved the lowest value of 0.82 for PLA/PEG8. However, when the content of PEG increased to 12%, $I_{1384/1361}$ slightly increased. This rise represented a decrease in crystallinity, which was confirmed by DSC and XRD.

3.1.2 Crystallinity of the Blends

Further observation of PEG plasticization in the PLA matrix was conducted by evaluating the crystal formation by XRD (Fig. 2). The diffraction peaks at $2\theta = 12.5^\circ$, 14.8° , 16.7° , 19.1° , and 22.4° corresponded to the (103), (010), (200)/(110), (203), and (210) planes of the PLA homo α -crystalline, respectively [35,36]. No diffraction peak at $2\theta = 11.9^\circ$, corresponding to the stereocomplex (SC) crystal, was detected in the PLA or PEG-plasticized blends. This result is almost similar to that reported by Tsuji et al. [37,38], where only α -form crystallites of PLLA were detected in the PLLA-b-PDLLA polymers, regardless of the PLLA fraction.

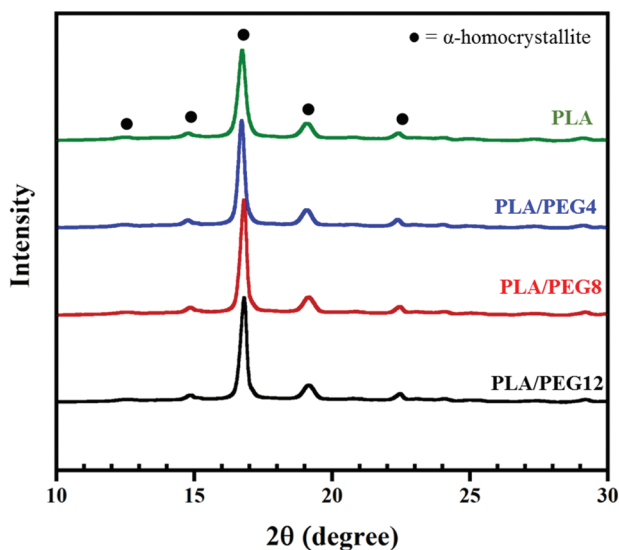


Figure 2: XRD diffractogram of PLA/PEG blends

In addition, the amount of PEG in our study does not affect SC formation. In contrast, a study [39] showed that the PEG in the PLLA/PDLA blends not only facilitates the crystallization of the PLLA matrix but also promotes SC crystal formation. Although PEG can act as a diluting agent in PLA blends, such that the interaction among PLA chains is reduced and the T_g is decreased, the content of D-lactic acid in our PDLA may be too low.

From the XRD results, the crystallinity index was also quantified. Fig. 3 reveals that the increase of crystallinity index for 0 to 8 wt% PEG blends occurred stably from 36.71% to 40.18%. This suggests that PEG plasticized the PLA chains based on the lubrication theory. PEG caused the PLA chains to move more easily by reducing the friction between intermolecular polymer chains [40]. As a result, after going through the formation of crystal nuclei in the solidification process, PLA chains were more prone to undergo a chain folding process, which consequently increased the index of crystallinity [41,42]. This

evidence supports the decrease of $I_{1384/1361}$ (as shown in Fig. 1C) that was observed when PEG was added up to 8 wt%.

Interestingly, the crystallinity decreased to 37.32% for PLA/PEG12. The decrease of crystallinity is in accordance with the increased $I_{1384/1361}$, suggesting an increase in the amount of amorphous chain regions.

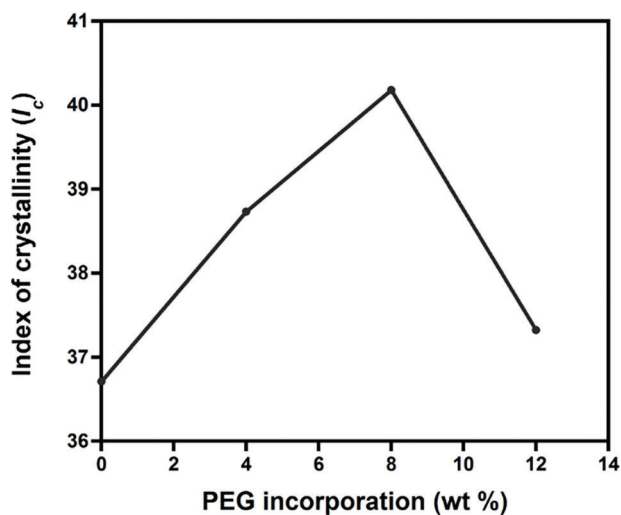


Figure 3: Effect of PEG incorporation to the index of crystallinity (I_c) of PLA/PEG blends

3.1.3 Thermal Behavior

Fig. 4 shows DSC thermograms of pure PLLA, PDLLA, PLA blends, and PEG-plasticized PLA blends, and Table 1 summarizes their thermal parameters. Pure PDLLA exhibited completely amorphous behavior [43] in which the T_g is observed at 45.1°C, and neither the melting temperature (T_m) nor crystallization temperature (T_c) nor cold crystallization temperature (T_{cc}) were detected. Pure PLLA showed a relatively high T_g at 74.9°C, which may be due to its low molecular weight. Upon blending with PDLLA, a single T_g is observed, and the value decreases to 51.9°C. This result agrees with Pan et al. [44], who reported that mixing PLLA with PDLLA ($X_{PDLLA} = 0.25$) lowered the T_g . This is attributed to the effect of stereoregularity on the helical conformation of PLA blends, which depends on the content of L-lactic acid units. For the PLLA/PDLLA blends (e.g., the fraction of D-lactic acid decreases), as the stereoregularity decreases, the T_g value decreases [44,45].

As seen in Table 1, all the blends with increasing fractions of PEG exhibited a single T_g peak that shifted to a low temperature. Plasticization using 4 wt% of PEG drastically reduced the T_g to 35.19°C, and an increase in PEG concentration proportionately reduced the T_g . The lowest T_g was achieved by PLA/PEG12 at 26.09°C, just below the ambient temperature. A similar trend was reported by Hu et al. [46], showing that the addition of PEG into PLA blends significantly decreased the T_g , and the content of 30% PEG yielded a T_g below the ambient temperature. These results indicate effective plasticizing by PEG and that the three components in the blend systems are miscible.

The incorporation of PEG up to 8% also led to an increase in T_c and crystallinity (X_c). This result suggested that PEG enhances the crystallization rate, thus increasing X_c , as shown in Table 1. However, the X_c decreased for PLA/PEG12. Higher contents of PEG may interfere with the crystallization process by disrupting PLA chains, which in turn leads to a decrease in crystallinity. Moradkhannejhad et al. [47] reported the same phenomenon for PEG in the PLA/curcumin blend, where the crystallinity decreased. The degree of crystallinity generated from the DSC data has a trend similar to that produced from FTIR

(Fig. 1C) and XRD (Fig. 3), in which the crystallinity showed an increase up to 8% PEG and then decreased at 12% PEG. The difference in value between I_c and X_c was mainly related to the different characterization methods. In addition, double melting peaks appeared upon PEG incorporation, revealing the polymorphic structures of δ and α crystals [30,48].

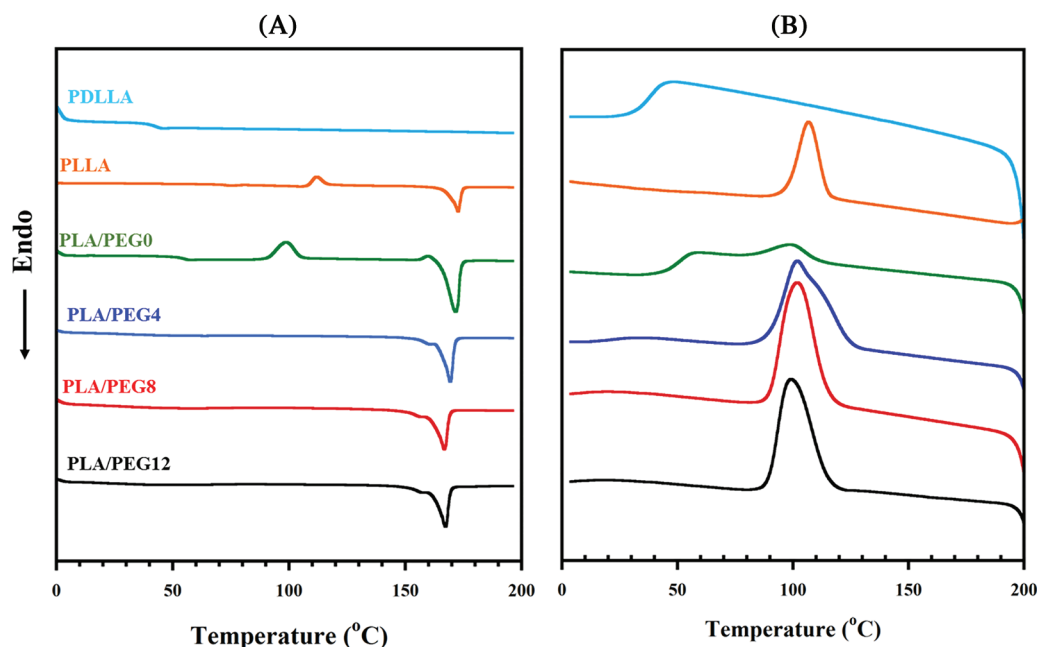


Figure 4: DSC thermograms of pure PDLLA, pure PLLA, PLA blends, and plasticized PLA blends during heating (A) and cooling (B)

Table 1: Thermal parameters of the blends obtained from the DSC thermograms

Samples	Heating					Cooling		
	T_g (°C)	T_{cc} (°C)	ΔH_{cc} (J/g)	T_m (°C)	ΔH_m (J/g)	T_c (°C)	ΔH_c (J/g)	X_c (%)
PDLLA	45.1	–	–	–	–	–	–	–
PLLA	74.9	111.8	14.2	172.7	32.8	106.8	26.4	19.9
PLA/PEG0	51.9	98.9	23.7	174.2	50.2	97.8	19.5	40.5
PLA/PEG4	35.2	–	–	169.2; 169.2	40.2	101.9	31.6	63.7
PLA/PEG8	29.0	–	–	155.8; 166.6	42.2	102.0	34.6	69.4
PLA/PEG12	26.1	–	–	155.7; 167.1	40.1	99.1	31.8	68.5

3.1.4 Microstructure Morphology of PLA/PEG Blends

SEM micrographs of the plasticized blends are presented in Fig. 5. Smooth ductile morphology was observed in PLA blends (Fig. 5A) and plasticized blends (Figs. 5B–5D), indicating that PEG is mixed homogeneously in the PLA matrix. PLA/PEG8 showed a smooth surface with some micro cracks (denoted by a blue arrow). On PLA/PEG12, a wider crack formation was visible, as seen in Fig. 5D. This

microcrack may have developed upon quenching the specimen in liquid nitrogen for sample preparation of SEM. The cryo-fracture may have caused the phase separation between PLA and PEG, generating the observed microcracks.

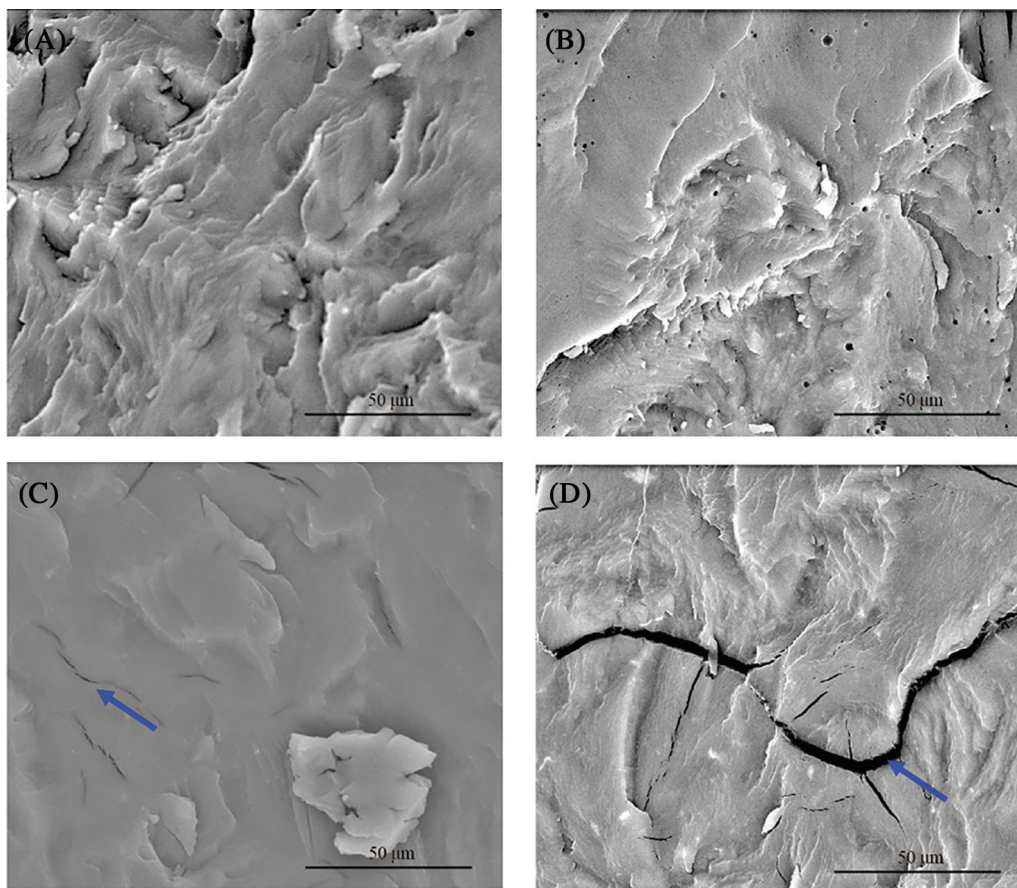


Figure 5: SEM micrographs of (A) PLA, (B) PLA/PEG4, (C) PLA/PEG8, and (D) PLA/PEG12

3.1.5 Hardness Properties of PLA/PEG Blends

Chain lubrication on the surface was further confirmed by the hardness of the blends (Fig. 6). The incorporation of PEG (4 wt%) significantly reduced the hardness from 24 HV to 10 HV. This is due to the lubricating ability of PEG, which is consistent with a significant reduction of T_g upon the addition of PEG (Table 1). PLA/PEG8 possessed a slightly lower hardness value of 7.88 HV. Further addition of PEG at 12 wt% reduced the hardness on the surface to 4.76 HV. This phenomenon occurred because the interaction of the polymer chain is weakened by the insertion of the PEG as a plasticizer [49].

3.2 *In vitro* Degradation Behavior of PLA/PEG Blends

3.2.1 Weight Loss

The hydrolytic degradation was evaluated by immersion of the specimens in PBS and incubating at 37°C, which resembles the physiological temperature of the human body. As seen in Fig. 7, the weight loss generally increased as the content of PEG increased. For the PLA and PLA/PEG4 blends, the weight loss was not observable in the first 7 days. In contrast, PLA/PEG8 lost weight by approximately 0.28%, and PLA/PEG12 experienced the highest mass loss, around 1.5%, on day 7. Then, the hydrolytic

degradation of all blends progressed further, as indicated by the increasing weight loss from time to time, with PLA/PEG12 showing the most significant mass reduction. The blends with a high content of PEG are more hydrophilic than those with lower contents [47]. This is because PEG is easily dissolved in water, especially PEG with low molecular weight. Therefore, PLA/PEG12 can easily lose PEG content during immersion in PBS. This result is in accordance with Kim et al. [50], reporting that the degradation rate rose with increasing the PEG content in PLLA.

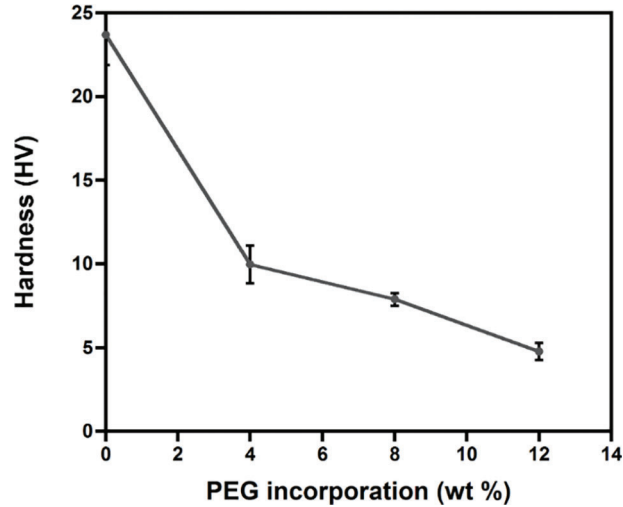


Figure 6: Effect of PEG incorporation on the hardness of PLA blends

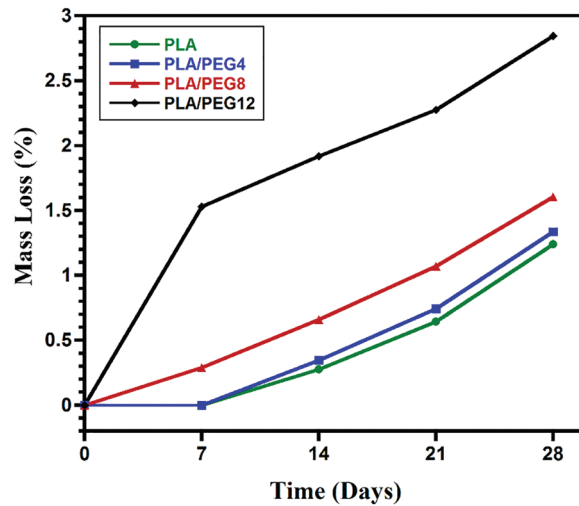


Figure 7: *In vitro* degradation of PLA/PEG blends for 28 days

3.2.2 Evolution of PLA Blends States of Order during *in Vitro* Degradation

The evolution of PLA blends state of order during *in vitro* degradation is evaluated using FTIR, particularly at the bands of 1384 and 1361 cm^{-1} , where the increase in the intensity ratio $I_{1384/1361}$ represents the increase of amorphous segments according to Dou et al. [33]. For the PLA blend without plasticizer, the weight loss in the first 14 days may indicate the degradation of amorphous PDLA

segments, leaving the crystalline PLLA chains. Thus, the decrease in $I_{1384/1361}$ is observed, as seen in Fig. 8. Tsuji et al. [51] studied the hydrolytic degradation of PDLLA/PLLA blends and found that PDLLA was largely degraded and removed from the blends, and thus the degradation rate of blends was elevated by the addition of PDLLA. The intensity ratio then rose again at 28 days, indicating the increase of amorphous segments due to the swelling of the crystalline PLLA chains by water penetration.

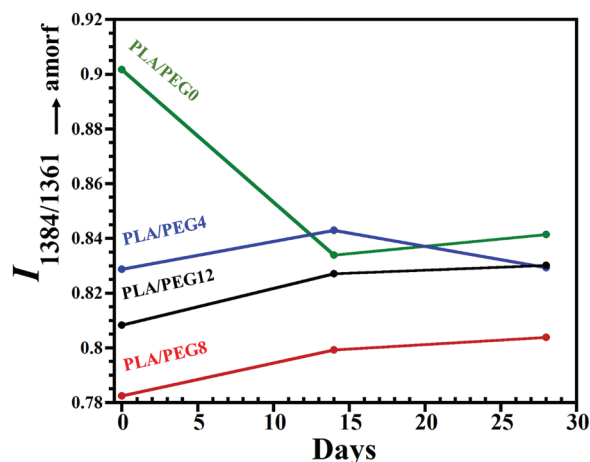


Figure 8: The variation of the intensity ratios $I_{1384/1361}$ for PLA and PLA/PEG blends during *in vitro* degradation

In contrast, for all plasticized PLA blends, the $I_{1384/1361}$ increased gradually in the first 14 days, which indicated the increase of amorphous segments. The presence of PEG assisted the mobility of the molecular chains of PLLA through swelling, increasing the free volume between the molecular chains and thus leading to the increase of amorphous PLLA. For PLA/PEG8 and PLA/PEG12, $I_{1384/1361}$ kept rising from 14 to 28 days, suggesting a further increase in the amorphous area, which was probably caused by re-swelling of the crystalline chains.

Meanwhile, for PLA/PEG4, a slight decrease of $I_{1384/1361}$ was observed at 28 days. This suggested that the PEG had completely dissolved in the water, inducing the decomposition of the amorphous chain and thereby increasing the crystalline segments.

In several reports, the hydrolytic degradation of PLA tended to increase the degree of crystallinity [52]. However, our results showed that all the plasticized blends experienced a decrease in crystallinity during the first 14 days of hydrolytic degradation. The analysis of $I_{1384/1361}$ may be more sensitive to the changes in PLLA chain ordering [33].

4 Conclusions

This study evaluated the effects of PEG incorporation on the physicochemical and degradation behavior of PLA blends. The conclusions can be expressed as follows:

1. The addition of PEG up to 8 wt% into PLA blends increased the crystallinity because of the plasticization effect of PEG. At 12 wt% PEG, the crystallinity decreased, which was attributed to the increase in amorphous segments. The DSC data indicated that PLA/PEG blends were miscible up to 12 wt% PEG. The XRD data revealed that no stereocomplex crystallites were observed, only homocrystallites. The increase of PEG content progressively decreased the hardness of the blends.

2. The *in vitro* degradation behavior showed that the increase in PEG content generally enhanced the degradation rate. In this case, PLA/PEG12 experienced the highest weight loss during 28 days of immersion.
3. The analysis of $I_{1384/1361}$ from the FTIR study provided an overview of structural evolution during hydrolytic degradation. Without PEG, the blends exhibited an increase in crystallinity during the first 14 days of degradation. In contrast, PEG-plasticized blends experienced a decrease in crystallinity during the first 14 days of degradation, owing to the effective plasticization by PEG.

Funding Statement: This work was supported by Universitas Indonesia under Grant PUTI 2020 (No. NKB-4325/UN2.RST/HKP.05.00/2020).

Conflicts of Interest: The authors declare that they have no conflicts of interest to report regarding the present study.

References

1. Liu, S., Qin, S., He, M., Zhou, D., Qin, Q. et al. (2020). Current applications of poly(lactic acid) composites in tissue engineering and drug delivery. *Composites Part B: Engineering*, 199, 108238. <https://doi.org/10.1016/j.compositesb.2020.108238>
2. Ju, J., Peng, X., Huang, K., Li, L., Liu, X. et al. (2019). High-performance porous PLLA-based scaffolds for bone tissue engineering: Preparation, characterization, and *in vitro* and *in vivo* evaluation. *Polymer*, 180, 121707. <https://doi.org/10.1016/j.polymer.2019.121707>
3. Singhvi, M. S., Zinjarde, S. S., Gokhale, D. V. (2019). Polylactic acid: Synthesis and biomedical applications. *Journal of Applied Microbiology*, 127(6), 1612–1626. <https://doi.org/10.1111/jam.14290>
4. Huang, W. Y., Hibino, T., Suye, S., Fujita, S. (2021). Electrospun collagen core/poly-L-lactic acid shell nanofibers for prolonged release of hydrophilic drug. *RSC Advances*, 11(10), 5703–5711. <https://doi.org/10.1039/D0RA08353D>
5. DeStefano, V., Khan, S., Tabada, A. (2020). Applications of PLA in modern medicine. *Engineered Regeneration*, 1, 76–87. <https://doi.org/10.1016/j.engreg.2020.08.002>
6. Dhanvantri, V., Ramya, R., Cherian, K. M., Ramesh, B. (2019). Evaluation of human dental stem cell growth characteristics and cellular morphological changes in response to extracellular matrix nanotopography. *Clinical and Laboratorial Research in Dentistry*, 1–15. <https://doi.org/10.11606/issn.2357-8041.clrd.2019.160296>
7. Ikuta, Y., Nakasa, T., Sumii, J., Nekomoto, A., Adachi, N. (2021). Histopathological and radiographic features of osteolysis after fixation of osteochondral fragments using poly-L-lactic acid pins for osteochondral lesions of the talus. *The American Journal of Sports Medicine*, 49(6), 1589–1595. <https://doi.org/10.1177/03635465211001758>
8. Bockmann, B., Jaeger, E., Dankl, L., Nebelung, W., Frey, S. et al. (2022). A biomechanical comparison of steel screws versus PLLA and magnesium screws for the Latarjet procedure. *Archives of Orthopaedic and Trauma Surgery*, 142(6), 1091–1098. <https://doi.org/10.1007/s00402-021-03898-w>
9. Feng, P., Jia, J., Liu, M., Peng, S., Zhao, Z. et al. (2021). Degradation mechanisms and acceleration strategies of poly (lactic acid) scaffold for bone regeneration. *Materials & Design*, 210, 110066. <https://doi.org/10.1016/j.matdes.2021.110066>
10. Golan, O., Shalom, H., Kaplan-Ashiri, I., Cohen, S. R., Feldman, Y. et al. (2021). Poly(L-lactic acid) reinforced with hydroxyapatite and tungsten disulfide nanotubes. *Polymers*, 13(21), 3851. <https://doi.org/10.3390/polym13213851>
11. Li, B., Xiong, F., Yao, B., Du, Q., Cao, J. et al. (2020). Preparation and characterization of antibacterial dopamine-functionalized reduced graphene oxide/PLLA composite nanofibers. *RSC Advances*, 10(32), 18614–18623. <https://doi.org/10.1039/D0RA03224G>
12. Adeosun, S. O., Lawal, G. I., Gbenedor, O. P. (2014). Characteristics of biodegradable implants. *Journal of Minerals and Materials Characterization and Engineering*, 2(2), 88–106. <https://doi.org/10.4236/jmmce.2014.22013>

13. Rasselet, D., Caro-Bretelle, A. S., Taguet, A., Lopez-Cuesta, J. M. (2019). Reactive compatibilization of PLA/PA11 blends and their application in additive manufacturing. *Materials*, 12(3), 485. <https://doi.org/10.3390/ma12030485>
14. Leonés, A., Peponi, L., Lieblich, M., Benavente, R., Fiori, S. (2020). *In vitro* degradation of plasticized PLA electrospun fiber mats: Morphological, thermal and crystalline evolution. *Polymers*, 12(12), 2975. <https://doi.org/10.3390/polym12122975>
15. Lascano, D., Moraga, G., Ivorra-Martinez, J., Rojas-Lema, S., Torres-Giner, S. et al. (2019). Development of injection-molded polylactide pieces with high toughness by the addition of lactic acid oligomer and characterization of their shape memory behavior. *Polymers*, 11(12), 2099. <https://doi.org/10.3390/polym11122099>
16. Takayama, T., Todo, M. (2006). Improvement of impact fracture properties of PLA/PCL polymer blend due to LTI addition. *Journal of Materials Science*, 41(15), 4989–4992. <https://doi.org/10.1007/s10853-006-0137-1>
17. Vieira, A. C., Vieira, J. C., Ferra, J. M., Magalhães, F. D., Guedes, R. M. et al. (2011). Mechanical study of PLA-PCL fibers during *in vitro* degradation. *Journal of the Mechanical Behavior of Biomedical Materials*, 4(3), 451–460. <https://doi.org/10.1016/j.jmbbm.2010.12.006>
18. Fortelny, I., Ujčić, A., Fambri, L., Slouf, M. (2019). Phase structure, compatibility, and toughness of PLA/PCL blends: A review. *Frontiers in Materials*, 6, 206. <https://doi.org/10.3389/fmats.2019.00206>
19. Eppley, B. L., Morales, L., Wood, R., Pensler, J., Goldstein, J. et al. (2004). Resorbable PLLA-PGA plate and screw fixation in pediatric craniofacial surgery: Clinical experience in 1883 patients. *Plastic and Reconstructive Surgery*, 114(4), 850–856. <https://doi.org/10.1097/01.PRS.0000132856.69391.43>
20. Yoon, S. K., Yang, J. H., Lim, H. T., Chang, Y. W., Ayyoob, M. et al. (2020). *In vitro* and *in vivo* biosafety analysis of resorbable polyglycolic acid-poly(lactic acid) block copolymer composites for spinal fixation. *Polymers*, 13(1), 29. <https://doi.org/10.3390/polym13010029>
21. Dell'Erba, R., Groeninckx, G., Maglio, G., Malinconico, M., Migliozi, A. (2001). Immiscible polymer blends of semicrystalline biocompatible components: Thermal properties and phase morphology analysis of PLLA/PCL blends. *Polymer*, 42(18), 7831–7840. [https://doi.org/10.1016/S0032-3861\(01\)00269-5](https://doi.org/10.1016/S0032-3861(01)00269-5)
22. Patrício, T., Bártolo, P. (2013). Thermal stability of PCL/PLA blends produced by physical blending process. *Procedia Engineering*, 59, 292–297. <https://doi.org/10.1016/j.proeng.2013.05.124>
23. Sakai, F., Nishikawa, K., Inoue, Y., Yazawa, K. (2009). Nucleation enhancement effect in poly(L-lactide) (PLLA)/poly(ϵ -caprolactone) (PCL) blend induced by locally activated chain mobility resulting from limited miscibility. *Macromolecules*, 42(21), 8335–8342. <https://doi.org/10.1021/ma901547a>
24. Casalini, T., Rossi, F., Castrovinci, A., Perale, G. (2019). A perspective on polylactic acid-based polymers use for nanoparticles synthesis and applications. *Frontiers in Bioengineering and Biotechnology*, 7, 259. <https://doi.org/10.3389/fbioe.2019.00259>
25. Tsuji, H. (2005). Poly(lactide) stereocomplexes: Formation, structure, properties, degradation, and applications. *Macromolecular Bioscience*, 5(7), 569–597. [https://doi.org/10.1002/\(ISSN\)1616-5195](https://doi.org/10.1002/(ISSN)1616-5195)
26. Chen, C. C., Chueh, J. Y., Tseng, H., Huang, H. M., Lee, S. Y. (2003). Preparation and characterization of biodegradable PLA polymeric blends. *Biomaterials*, 24(7), 1167–1173. [https://doi.org/10.1016/S0142-9612\(02\)00466-0](https://doi.org/10.1016/S0142-9612(02)00466-0)
27. Choi, S. H., Lee, J. H. (2016). Absorbable plate-related infection after facial bone fracture reduction. *Archives of Craniofacial Surgery*, 17(1), 1–4. <https://doi.org/10.7181/acfs.2016.17.1.1>
28. Kang, H., Li, Y., Gong, M., Guo, Y., Guo, Z. et al. (2018). An environmentally sustainable plasticizer toughened polylactide. *RSC Advances*, 8(21), 11643–11651. <https://doi.org/10.1039/C7RA13448G>
29. Nashchekina, Y., Nikonov, P., Nashchekin, A., Mikhailova, N. (2020). Functional polylactide blend films for controlling mesenchymal stem cell behaviour. *Polymers*, 12(9), 1969. <https://doi.org/10.3390/polym12091969>
30. Yu, Y., Cheng, Y., Ren, J., Cao, E., Fu, X. et al. (2015). Plasticizing effect of poly(ethylene glycol)s with different molecular weights in poly(lactic acid)/starch blends. *Journal of Applied Polymer Science*, 132(16), 41808. <https://doi.org/10.1002/app.41808>

31. Li, F. J., Zhang, S. D., Liang, J. Z., Wang, J. Z. (2015). Effect of polyethylene glycol on the crystallization and impact properties of polylactide-based blends. *Polymers for Advanced Technologies*, 26(5), 465–475. <https://doi.org/10.1002/pat.3475>
32. Al-Sukhun, J., Törnwall, J., Lindqvist, C., Kontio, R. (2006). Bioresorbable poly-l/dl-lactide (P[L/DL]LA 70/30) plates are reliable for repairing large inferior orbital wall bony defects: A pilot study. *Journal of Oral and Maxillofacial Surgery*, 64(1), 47–55. <https://doi.org/10.1016/j.joms.2005.09.013>
33. Dou, T., Zhou, B., Hu, S., Zhang, P. (2021). Evolution of the structural polymorphs of poly(l-lactic acid) during the *in vitro* mineralization of its hydroxyapatite nanocomposites by attenuated total reflection fourier transform infrared mapping coupled with principal component analysis. *Polymer*, 236, 124318. <https://doi.org/10.1016/j.polymer.2021.124318>
34. Chen, H., Du, X., Yang, A., Yang, J., Huang, T. et al. (2014). Effect of graphene oxides on thermal degradation and crystallization behavior of poly(l-lactide). *RSC Advances*, 4(7), 3443–3456. <https://doi.org/10.1039/C3RA45480K>
35. Dai, S., Wang, M., Zhuang, Z., Ning, Z. (2020). Crystallization and alkaline degradation behaviors of poly(l-lactide)/4-armed poly(ϵ -caprolactone)-block-poly(d-lactide) blends with different poly(d-lactide) block lengths. *Polymers*, 12(10), 2195. <https://doi.org/10.3390/polym12102195>
36. Shao, J., Xiang, S., Bian, X., Sun, J., Li, G. et al. (2015). Remarkable melting behavior of PLA stereocomplex in linear PLLA/PDLA blends. *Industrial & Engineering Chemistry Research*, 54(7), 2246–2253. <https://doi.org/10.1021/ie504484b>
37. Tsuji, H., Iguchi, K., Tashiro, K., Arakawa, Y. (2020). Crystallization behavior, structure, morphology, and thermal properties of crystalline and amorphous stereo diblock copolymers, poly(L-lactide)-b-poly(DL-lactide). *Polymer Chemistry*, 11(36), 5711–5724. <https://doi.org/10.1039/D0PY01115K>
38. Tsuji, H., Iguchi, K., Arakawa, Y. (2021). Stereocomplex- and homo-crystallization behavior, structure, morphology, and thermal properties of crystalline and amorphous stereo diblock copolymers, enantiomeric poly(l-lactide)-b-poly(dl-lactide) and poly(d-lactide)-b-poly(dl-lactide). *Polymer*, 213, 123226. <https://doi.org/10.1016/j.polymer.2020.123226>
39. Song, Y., Wang, D., Jiang, N., Gan, Z. (2015). Role of PEG segment in stereocomplex crystallization for PLLA/PDLA-b-PEG-b-PDLA blends. *ACS Sustainable Chemistry and Engineering*, 3(7). <https://doi.org/10.1021/acssuschemeng.5b00214>
40. Marcilla, A., Beltrán, M. (2017). Mechanisms of plasticizers action. In: Wypych, G. (Ed.), *Handbook of plasticizers*, 2nd edition, vol. 3, pp. 119–134. Amsterdam: Elsevier. <https://doi.org/10.1016/B978-1-895198-97-3.50007-X>
41. Ma, Z., Yang, P., Zhang, X., Jiang, K., Song, Y. et al. (2019). Quantifying the chain folding in polymer single crystals by single-molecule force spectroscopy. *ACS Macro Letters*, 8(9), 1194–1199. <https://doi.org/10.1021/acsmacrolett.9b00607>
42. Xu, H., Yang, X., Xie, L., Hakkarainen, M. (2016). Conformational footprint in hydrolysis-induced nanofibrillation and crystallization of poly(lactic acid). *Biomacromolecules*, 17(3), 985–995. <https://doi.org/10.1021/acs.biomac.5b01636>
43. El-Hadi, A. M. (2019). Miscibility of crystalline/amorphous/crystalline biopolymer blends from PLLA/PDLA/PHB with additives. *Polymer-Plastics Technology and Materials*, 58(1), 31–39. <https://doi.org/10.1080/03602559.2018.1455863>
44. Pan, P., Liang, Z., Zhu, B., Dong, T., Inoue, Y. (2009). Blending effects on polymorphic crystallization of poly(l-lactide). *Macromolecules*, 42(9), 3374–3380. <https://doi.org/10.1021/ma8024943>
45. Urayama, H., Moon, S. I., Kimura, Y. (2003). Microstructure and thermal properties of polylactides with different L- and D-unit sequences: Importance of the helical nature of the L-sequenced segments. *Macromolecular Materials and Engineering*, 288(2), 137–143. <https://doi.org/10.1002/mame.200390006>
46. Hu, Y., Rogunova, M., Topolkarayev, V., Hiltner, A., Baer, E. (2003). Aging of poly(lactide)/poly(ethylene glycol) blends. Part I. Poly(lactide) with low stereoregularity. *Polymer*, 44(19), 5701–5710. [https://doi.org/10.1016/S0032-3861\(03\)00614-1](https://doi.org/10.1016/S0032-3861(03)00614-1)

47. Moradkhannejhad, L., Abdouss, M., Nikfarjam, N., Shahriari, M. H., Heidary, V. (2020). The effect of molecular weight and content of PEG on *in vitro* drug release of electrospun curcumin loaded PLA/PEG nanofibers. *Journal of Drug Delivery Science and Technology*, 56, 101554. <https://doi.org/10.1016/j.jddst.2020.101554>
48. Cheng, L., Hu, C., Li, J., Huang, S., Jiang, S. (2019). Stereocomplex-affected crystallization behaviour of PDLA in PDLA/PLDLA blends. *CrystEngComm*, 21(2), 329–338. <https://doi.org/10.1039/C8CE01934G>
49. Norazlina, H., Kamal, Y. (2021). Elucidating the plasticizing effect on mechanical and thermal properties of poly (lactic acid)/carbon nanotubes nanocomposites. *Polymer Bulletin*, 78(12), 6911–6933. <https://doi.org/10.1007/s00289-020-03471-2>
50. Kim, Y., Son, S., Chun, C., Kim, J. T., Lee, D. Y. et al. (2016). Effect of PEG addition on pore morphology and biocompatibility of PLLA scaffolds prepared by freeze drying. *Biomedical Engineering Letters*, 6(4), 287–295. <https://doi.org/10.1007/s13534-016-0241-3>
51. Tsuji, H., Ikada, Y. (1997). Blends of crystalline and amorphous poly(lactide). III. Hydrolysis of solution-cast blend films. *Journal of Applied Polymer Science*, 63(7), 855–863. [https://doi.org/10.1002/\(ISSN\)1097-4628](https://doi.org/10.1002/(ISSN)1097-4628)
52. Elsayy, M. A., Kim, K. H., Park, J. W., Deep, A. (2017). Hydrolytic degradation of polylactic acid (PLA) and its composites. *Renewable and Sustainable Energy Reviews*, 79, 1346–1352. <https://doi.org/10.1016/j.rser.2017.05.143>